Experiments on Ballooning in Pressurized and Transiently Heated Zircaloy-4 Tubes

M. E. Markiewicz, F. J. Erbacher
Institut für Material- und Festkörperforschung
Institut für Reaktorbauelemente
Projektgruppe LWR-Sicherheit

Kernforschungszentrum Karlsruhe

KERNFORSCHUNGSZENTRUM KARLSRUHE

Institut für Material- und Festkörperforschung
Institut für Reaktorbauelemente
Projektgruppe LWR-Sicherheit

KfK 4343

EXPERIMENTS ON BALLOONING IN PRESSURIZED AND

TRANSIENTLY HEATED ZIRCALOY-4 TUBES

M.E. Markiewicz*, F.J. Erbacher

*Comision Nacional de Energia Atomica
Centro Atomico Constituyentes, Buenos Aires

Abstract

Single-rod burst tests were performed with Atucha I Zircaloy-4 cladding tubes in the REBEKA burst equipment of KfK. The objective was to investigate the ballooning and burst behavior of argentine cladding tubes obtained from NRG , Germany and CONVAR, Argentina. The burst data were compared with those of cladding tubes used in german PWR's.

It was found that the burst data e.g. burst temperature, circumferential burst strain and its response to azimuthal temperature differences are identical for the argentine and german tubing quality. The burst data are in good agreement with those of german PWR-Zircaloy tubes. Thus, the fuel rod behavior codes developed for german PWR's can also be used for the argentine reactor Atucha I.

Zusammenfassung

Berstversuche an innendruckbeaufschlagten und transient beheizten Zircaloy-4 Rohren.

In der Einzelstabberstversuchsanlage REBEKA wurden Berstversuche an Zircaloy-4 Hüllrohren des argentinischen Kernkraftwerkes Atucha I durchgeführt.

Zielsetzung der Versuche war die Untersuchung des Verformungs- und Berstverhaltens argentinischer Hüllrohre aus deutscher (NRG) und argentinischer (CONVAR) Herstellung. Die Berstdaten wurden mit denen von Zircaloy-Hüllrohren deutscher Druckwasserreaktoren verglichen.

Ein Vergleich der ermittelten Berstdaten wie z.B. Bersttemperatur, Berstumfangsdehnung und deren Beeinflussung durch azimutale Temperaturunterschiede ergab, daß kein Unterschied zwischen der deutschen und argentinischen Rohrqualität besteht und die Berstdaten gut mit denen der Zircaloy-Hüllrohre deutscher Druckwasserreaktoren übereinstimmen. Dies bedeutet, daß die für deutsche Reaktoren entwickelten Brennstabversagenscodes auch für Atucha I verwendet werden können.

Contents

List of Tables

1. Introduction

The majority of Pressurized Water Reactors (PWR) uses Zircaloy-4 material as fuel claddings which are prepressurized with helium gas during manufacturing.

If a loss-of-coolant-accident (LOCA) occurs, coolant depressurization can take place in a few seconds, depending on the break size. This rapid depressurization creates an increasing internal to external pressure differential which gives rise to an increasing biaxial stress in the clad.

Concurrently the decreased heat transfer caused by loss-of-coolant causes the clad temperature to increase. Later on, stress-temperature combination reaches a point where the clad begins to increase in diameter and then to deform locally. This local plastic deformation (ballooning) was identified as the failure mechanism, and it is a consequence of elevated cladding temperature which reduces the strength of the material combined with an increase in stress caused by the internal overpressure after coolant depressurization. Such deformation can cause partial channel blockage in the fuel elements and may impair the efficiency of the emergency cooling.

Thus cladding temperature and differential pressures are the primary parameters that determine cladding circumferential strain during ballooning.

For the failure analysis within the licensing procedure, the clad expansion and rupture characteristic and its influence on the emergency core cooling must be known. For this reason and for a better understanding of the high-temperature deformation and rupture behaviour of Zircaloy cladding, transient temperature burst tests were made.

The transient tests concentrate on the simulation of the second heatup phase of a LOCA. During this phase, the probability of failure is considered to be higher than in other phases because of the relatively long time the cladding is at high temperatures while the internal overpressure causes elevated stress in the cladding [1].

2. Objectives

This work presents the results of an investigation of how Zircaloy-4 clad behaves when subjected to temperatures and differential pressures.

The prime objectives of these experiments are:

a) to obtain information on the ballooning characteristics of the Argentine Zircaloy-4 cladding under specified internal pressures, temperatures and temperatures-non-uniformities.

b) to establish a quantitative difference with the clads fabricated by NRG.

c) Incorporate the mechanical properties information into fuel-modelling codes that will provide a quantitative basis for evaluating cladding deformation over a range of LOCA.

3. Material apparatus and experimental procedures

The experiments were carried out in the REBEKA single rod test equipment of KfK in the IRB institute.

Transient tests were performed on single PWR-size Zircaloy-4 tubes at a variety of internal pressures and temperatures to establish data with reference to LOCA and materials parameters.

Tests were run with internal pressure from 6.5 to 98 bar and with a nominal heating rate of 1 °C/sec. The amount of circumferential expansion, amount of wall thinning, axial length change, rupture temperature and physical appearance of the tubing for each experiment were determined.

The tests were limited to two controlled independent variables: internal pressure and heating rate. The dependent variables were rupture temperature, time to rupture, circumferential and wall thickness strain, and the physical appearance of the ruptured tubing.

The Zircaloy-4 cladding used in this work was obtained form NRG (Germany) and CONVAR (Argentina), and they are for normal use in PHWR Atucha I.

The nominal outside diameter was 11.9 mm by 0.55 mm wall thickness. All the specimens were 500 mm long with an internal heated length of approximately 325 mm.

A stack of alumina annular pellets (Al_2O_3) was used to simulate the fuel column in a fuel elements. The diametral clearance between the I.D. of the cladding and the O.D. of the pellets was 0.15 mm. The axial gap distance between the end plugs and alumina pellets stack was 15 mm. Considering this magnitude and the change in the axial length of the tube, it can be said that these experiments were carried out under axially unconstrained conditions.

The Zircaloy cladding was heated indirectly by conduction heating from inside using an electrically insulated heater rod installed in the center. The Zircaloy cladding, the aluminium oxide pellets and the heater rod are assembled into the complete fuel rod simulator.

Figure 1 shows the schematic design of the fuel rod simulator.

The test apparatus consisted basically of a fuel rod simulator, a gas-handling system to pressurize the specimen, a steam generator and a programmable d.c. powder supply for indirect electrical heating of the tube, Figure 2 shows it schematically.

The signal from the four thermocouples (spot welded on the outer surface of the tube, one for control and three for measurement of the azimuthal temperature difference) and pressure transducer were continuously monitored and recorded on a computer.

Each test was initiated after the entire assembly was equilibrated at initial temperature condition of about 300 °C using the internal and shroud electrical heaters and superheated steam, also the helium pressure was adjusted to the desired value. Earlier tests [2] showed that there was no difference in behaviour between specimens heated from room temperature and specimens preheated to 300 °C before the temperature ramp.

The tests were terminated just after rupture by cutting the power. A typical recording of the transient test is presented in Figure 3.

In some of the tests, X-ray cinematography with a high-speed camera was used to record the diametral change of the tube during the burst test, the camera frames were magnified in an optical microscope and then the measurements were used to calculate the diametral strain. This was important because it gives an information of the strain on the ballooning as function of time.

Circumferential strain was measured by wrapping a piece of Scotch tape around the tube at the rupture, marking the tape at the rupture edges, removing the tape, and measuring the circumference from one edge of the rupture around to the other.

Circumferential strain was defined as:

$$\left(\frac{L_f}{L_0} - 1\right) \cdot 100$$

where
L_f = final length
L_0 = initial circumference

Finally, each tube was sectioned through the region of maximum expansion and the remaining wall thickness was measured.

Only in four tests the thermocouple location resulted in preferential burst sites, such tests were not considered in the results.

4.   Results
4.1   Tests with uniform temperature distribution

A large number of single burst transient tests have been performed in the past [3,4] on Zircaloy-4 cladding, with 10.75 mm o.d. and 0.725 mm wall thickness. The present test results are consistent with them; the burst data, i.e., burst temperature, burst pressure, maximum circumferential strain at the rupture location, axial strain, engineering burst stress and time to burst, are listed in Table 1 and 2 for the Argentine and NRG tubes, respectively.

The information obtained on the circumferential strain at failure as a function of burst temperature, indicates the extreme sensitivity of such deformation on

temperature, showing in the range investigated two maximum strains at ~ 800 and ~ 960 °C, with a minimum in the alpha plus beta phase transition. This is illustrated in Figure 4 where the maximum diametral expansion is plotted versus the burst temperature.

Although the exact mechanisms responsible for the large circumferential strain peak near 800 °C is not clear, M. Chung [5] supposes that grain boundary sliding of equiaxed α grain may play a significant role in addition to deformation by dislocation glide.

In this high α phase range temperature, Zircaloy which has a strong radially texture, shows a specific deformation behaviour due to its texture and aniso-tropy. The circumferential elongation is accompanied to some extent by remark-able tube shortening since the tube resists accommodation of tangential expansion solely by deformation in the radial direction (wall thinning). The observed change in tube length is plotted in Figure 5 as a function of burst temperature.

The axial strain was determined measuring the change on the effective cladding length after the test and related only to a length of 60 mm. Such shrinkage in the cladding length shows a maximum in the high α phase range which is nearly coincident with the temperature for the maximum in the circumferential stain.

Invariably, for the tests at higher temperatures, a net elongation was observed in the α + β and β phase range, this is understood since β-Zircaloy, being essentially isotropic, accommodates deformation primarily by wall thinning due to a combination of factors such as axial force (pressure) and perhaps oxide volume change [6].

It is clear that the α to β phase transformation has a considerable influence on the deformation of Zircaloy-4 tubing. The minimum in the rupture ductility in this range at approximately 900 °C (Figure 4), gave a total circumferential elongation value of 45 %. Some investigators attribute the diminution in the ductility as a lack in the work hardening in this range.

The second maximum of strain occurs in the upper α + β range with a circumferential deformation of 68 % at 960 °C.

At higher burst temperature the circumferential expansion decreases sharply as a result of the significant amount of oxidation associated with the low heating rate used in these experiments.

As will be dicussed later, additional weakening of the cladding is produced due to oxide cracking which leads to localized wall thinning. Transient burst experiments carried out in argon atmosphere [5], show that at these temperatures, around 1000 °C, the decrease in the rupture ductility does not exist, but increase till values higher than those reached in the α phase, as a consequence of oxidation inhibition.

Several works [7,8] demonstrated that the magnitude of the maximum and minimum in the circumferential strain and their temperatures are influenced by the heating rate as a consequence of the variation in the strain rate hardening in the tests made at lower temperature, and the amount of oxidation at higher temperatures.

Figure 6 shows the relationship between burst pressure and burst temperature. In many cases it is more useful to compare burst stresses rather than burst pressures, in order to eliminate dimensional effects. Therefore, the measured burst pressures were converted to burst stresses according to the relation give below, the results are listed in Table 1 and 2.

$$\sigma_B = P_B \cdot \frac{D_i}{2 t_0}$$

σ_B = engineering hoop stress

P_B = burst pressure

D_i = initial internal diameter

t_0 = initial wall thickness

Figure 6 shows that below ~ 820 °C (α to α + β transformation) is the range of temperature in which the Zircaloy cladding exhibits a relatively large decrease in strength as the temperature increases.

The appearance of the burst opening and lateral view of selected burst specimens are shown in Figure 7.

The amount of ballooning at the fracture, the shape of the burst opening and the difference in the cladding surface oxidation at higher temperatures can be clearly seen. An important observation of the photograph showing the lateral view is that the expansion was essentially symmetrical about the longitudinal axis and the tubes remained straight after the burst, some authors attribute part of the bending to be caused by escaping gas jet reaction at the moment of rupture. In the present tests, and in particular in those carried out at high pressure, where the stored gas energy is high, the tube did not bend. The casue for the observed tube bowing is believed to be mainly, as will be shown later, a consequence of non-uniform temperatures distributions which produce non-uniform axial contractions.

The axial extension of maximum deformation was limited on relatively small zones on the tube. The shape of the cladding is conical at both sides of the burst with a small strain over a considerable length.

Figure 8 shows quantitatively the axial distribution of the circumferential strain for four burst tubes. It is evident that tube A-3 with the highest circumferential elongation of 106 %, concentrated in a short axial length of 40 mm strains greater than 35 %.

The failure mode of the cladding was strongly influenced by the burst temperature. Two different failure modes were observed in the range of temperature between 700 and 1000 °C.

The specimens that ruptured in the α phase region, the rupture was violent and the opening area was big with nearly rectangular shape. For bursts in the $\alpha + \beta$ and low β phase, the burst opening was narrow with a very small area (Figure 7).

In a nuclear fuel rod the area of burst opening can influence the egress of fission products and possibly fuel fragments to the coolant as well as the ingress of steam to the inner surface of the cladding in a LOCA situation. Such areas were measured and represented versus the burst temperature in Figure 9.

The size of the opening increased with increasing burst pressure, with a maximum of 21 mm^2 in the $\alpha + \beta$ and low β phase and between 68 and 320 mm^2 for ruptures in the α phase. This reflects the influence of increase in stored energy on deformation during the burst.

4.2 Metallographic observation

Microstructural examination showed a large difference in the rupture region of specimens burst in α phase or in α + β and β phase. The rupture edge of specimens which burst below 840 °C was characterized by a blunt edge typical of a shear process, whereas in those burst at higher temperatures, the fracture edge was sharp with a considerable thinning of the tube wall in the burst region.

Figure 10 shows the typical cross section photographs at the failure location of tubes burst in α + β and β phase.

The cross section at the burst location was examined for tubes that burst at temperatures below 840 °C and the true radial fracture strain was determined with the following relation:

$$\varepsilon_r = \ln \frac{t_a}{t_0}$$

ε_r = true rupture radial strain
t_a = thickness of the rupture tip
t_0 = initial cladding thickness

Due to the blunt rupture edge in the α range, the radial strain could be measured unambiguously and represented versus burst temperature in Figure 10. The results indicate more rupture wall thinning at higher temperatures.

Figure 11 is a plot of maximum wall thickness (opposite to burst) versus maximum circumferential deformation. The wall thickness measurements demonstrate, as expected, that the smallest values correspond for specimens with the highest expansion.

These results are important from the point of view of the amount of embrittlement in the cladding due to oxygen diffusion into the tube wall during a thermal excursion following a LOCA.

It is knonw that at high temperatures a significant amount of oxygen reacts with Zircaloy, this can cause appreciable changes in the metal strength and ductility. In the range of temperature investigated and considering the influence of steam

oxidation on the rupture ductility, the results can be divided in two groups with a transition point around 950 °C; below this temperature, the difference in the amount of oxidation seems to have not a large effect on ductility. A maximum of 12 μm for oxide plus oxygen stabilized α phase was measrued in specimen which reached 900 °C; after the test the oxide layer remained homogeneous and intact.

At temperatures above 950 °C, the zirconium oxide film showed many longitudinal cracks, the morphology and the amount of them seem to be related to temperature and time to exposure, this means to the amount of oxidation (see Figure 7, specimens burst at 958 and 1012 °C). Cross sections of such tubes are shown in Figure 12, the transversal cuts were made at the same circumferential strain of 15 %. The tube which burst at 958 °C shows a multitude of fine shallow cracks in the external surface, while the tube brust at 1012 °C shows the presence of fewer but deeper cracks with a reduced ability for ballooning.

A magnification of a small crack developed in specimen A-41, Figure 12, shows the oxide layer had cracked in a brittle manner producing a straigth side crack, a progressive opening of the crack is followed by oxidation of the exposed metal.

As the straining proceeds, the cracks extend into the central β phase of the tube increasing the local hoop stress. On the unoxidized inner surface, the material undergoes a considerable wall thinning in the vicinity or opposite to the cracks. Such a combination of wall necking from the inside surface and crack opening on the outside surface leads to a rapid failure with a dramatic reduction in the ductility. Typical cross sections, magnification of a necking zone and rupture tip of tube that burst at temperature in the β phase, are shown in Figure 13.

To illustrate the ballooning development with the time, four specimens were filmed with a high speed camera, the specimens choosen burst around 700, 800, 900 and 1000 °C; it is clear from Figure 14 that the total strain developed in a period of 10 seconds before rupture is less than 15 % and the abrupt change in the slop which lead to the localized strain is produced between 1 to 4 seconds before rupture. The specimen burst at the highest temperature (1012 °C) does not show such change in the strain rate due to a sudden rupture as a consequence of the oxidation effect discussed above.

4.3 Tests with azimuthal temperature difference

During refilling and reflooding phase of a LOCA, both axial and circumferential temperature differences are produced. To investigate the effect of temperature non-uniformity on the maximum circumferential expansion of Zircaloy cladding a series of transient-heating burst experiments were performed.

As was already said, the heating of the cladding is produced indirectly by an internal heater accompanied by a shroud heater tube which could be heated to produce uniform temperature on the cladding circumference. During the test with azimuthal temperature difference, the shroud heater was switched off, generating in this way a temperature difference around the cladding, due to the so produced external heat transfer combined with non-uniform gaps between the pellets and the cladding. Such temperatures were measured with three thermocouples resistance spot-welded to the outer clad surface at the same axial elevation and separated 120° between them. This method has some uncertainty in the determination of the location for maximum and minimum temperatures.

The variation in the circumferential temperature obtained with and without the shroud heater were within 3 °C (minimum) and 58 °C (maximum) respectively, for the Argentine cladding. Table 3 gives these values and the total strain. All the tests were conducted at the same constant internal pressure with a heating rate of 1 °C/sec; the temperature in the last part of each experiment was monitored each 0.1 sec, this small interval was due to the higher azimuthal temperature differences the cladding develops in the few seconds previous to the rupture due to the non-uniformity in the ballooning in this type of experiments.

As was already demonstrated [4,9] under azimuthal temperature conditions, representative of a LOCA, straining occurs first on the hot side. As a consequence the cladding will experience an axial shrinkage on that side caused by ansiotropy and will bow the cladding forcing it into close contact with the heat source on the hot side (where the burst occurs). The opposite cold side is deformed in such a way that it moves away from the heat source.

The temperature difference along the circumference will increase as the hot spot heats up and the opposite side cools down, in this way azimuthal temperature distribution on the cladding are intensified during deformation. Figure 3 shows a plot of a typical circumferential temperature distribution during the ballooning

process. Minor temperature difference can be found at the beginning of the experiment, reaching about 30 °C at rupture time. The two thermocouples located on the side opposite to the rupture point show a decreasing temperature rise as a function of time; the thermocouple located close to the rupture indicates a higher increase in the temperature up to the rupture time.

This tendency in the temperature difference is a demonstration that the cladding does not lift off the heat source on the hotter side where the tube ruptures.

Figure 15 clearly shows this behaviour for a specimen with high azimuthal temperature difference, while in the case of uniform temperature distribution around the circumference, the cladding remains straight.

As the deformation is very sensitive to temperature, the cladding circumferential strain and wall thinning becomes a function of the prevailing temperatures at different points of the circumference. This implies that the circumferential elongation is produced primarily by local weakening of the wall thickness concentrated to only a limited part of the entire circumference of the cladding. This localization of deformation at the hot spot gives rise to a relatively early burst at that point and avoids high average circumferential burst strain in spite of much larger local strain. This can be seen in Figure 16 which shows the tip and opposite burst orientation for two specimens tested with different azimuthal temperature difference.

Figure 17 is an indication of the influence of non-uniformities in the temperature around the circumference on the burst strain. The figure makes clear the great effect of such temperature variation on reducing the burst strain. Small azimuthal differences on the cladding produce a nearly uniform reduction of the wall thickness along the circumference and lead to a large circumferential burst strain, by other hand, large temperature variations lead to a localized reduction in wall thickness and hence to relatively low circumferential burst strain.

Variations of temperatures around the cladding of about 15 to 20 °C cause reductions of 50 % in the burst strain. Such abrupt drop in the deformation values continues up to the azimuthal temperature difference reaches around 30 °C. Beyond, the diminutions on the deformations, although it continues, is not as strong, for example, an increase of 100 % in the circumferential temperature

variation, from 30 to 60 °C produces a decrease in the burst strain from 35 to 25 %.

The azimuthal strain distribution is believed to be mainly caused by azimuthal temperature variation [10] rahter than by initial wall thickness variation or other effects.

Therefore, the local temperature non-uniformity was identified as a decisive parameter in relation to the ballooning strain.

4.4   Comparison of results with NRG cladding

One of the objectives of this work was to compare the behaviour of the Argentine cladding with the results obtained from tubes fabricated by NRG. For this motive the same test parameters were used, internal pressure and heating rate. This last one, and as was already said, seem to have a large effect on the results of burst strain and burst temperature. For this reason the data points of burst temperature versus time to burst were plotted in Figure 18 showing a good agreement among both types of cladding, the least square method gave a slope of 1.08 °C/sec which is in good concordance with the predetermined heating rate value of 1 °C/sec.

Figures 19, 20 and 21 show the results in comparison. Some differences are in the axial strain versus burst temperature (Figure 21). it was found that the NRG claddings do not present a minimum in the α phase as is in the case of the Argentine tubes. The reason could be the more flat curve of circumferential strain in the range of temperature between 700 to 800 °C, and perhaps small differences in texture due to fabrication.

Figure 22 is a comparison how the azimuthal temperature differences affect the circumferential strain in both claddings.

The influence of non-uniformities in the temperature on the circumferential burst strain is more pronounced in the Argentine tubes.

To underline and prove these minor differences, more experiments would be needed. However, out of these differences, the results showed a good agree-

ment, at least in the range of temperatures investigated and at the heating rate used.

5. Conclusions

- In the α phase range axial contraction of the cladding is significant, such shrinkage increases as the circumferential strain increases.

- The α to β transformation has a considerable influence on the strain behaviour, a reduction in the rupture ductility occurs in the middle of the α + β phase.

- Steam oxidation produces a significant reduction in the circumferential strain in the β phase as a consequence of cracks in the oxide layer.

- The degree of temperature uniformity is of great importance in the amount of deformation, the more uniform is the temperature, the greater is the deformation.

- Azimuthal temperature difference causes non-uniform axial contraction and tube bending and limits the total circumferential strain.

- A good agreement exists in the transient test results for the Argentine and NRG cladding in the range of temperature 700 to 1000 °C.

6. Comment

Transient test data published by Erbacher et al. [4] were used in the computer code system SSYST, which describes the transient fuel rod behaviour under LOCA conditions. A comparison of the present results with them shows a good concordance. This means that such a computer code system could be used also in the analysis of transient tests for the Argentine Atucha I tubes.

Acknowledgements

- 14 -

7. References

[1] E.H. Karb, M. Prüßmann et al.
"LWR Fuel Rod Behaviour in the FR2 In-Pile Test Simulating the Heatup Phase of a LOCA"
KfK-3346

[2] D.G. Hardy
"High temperature expansion and rupture behaviour of Zircaloy tubing"
Proceedings of Topical Meeting on Water Reactor Safety, Salt Lake City, Utah, March 26-28, 1973, CONF-730304, pp. 254-273

[3] A. Fiege
"Fuel behaviour under LOCA conditions"
Proc. of the second German-Finnish seminar on Nuclear Safety. Otaniemi, Finland, September 29-30, 1982, pp. 115-158

[4] F.J. Erbacher, S. Leistikow
"Zircaloy Fuel Cladding Behaviour in a LOCA"
Seventh international conference on Zirconium in the Nuclear Industry, 24-27 June, 1985, Strasbourg, France, ASTM-STP 939, pp. 451-488

[5] H.M. Chung, T.F. Kassner
"Deformation characteristics of Zircaloy claddings in vacuum and steam under transient-heating conditions"
NUREG/CR-0344 ANL-77-31

[6] R.H. Chapman, J.L. Crowley et al.
"Zirconium cladding deformation in steam environment with transient heating"
Zirconium in the Nuclear Industry, ASTM STP 681, American Society for Testing and Materials, 1979, pp. 393-408

[7] F.J. Erbacher
"LWR fuel cladding deformation in a LOCA and its interaction with emergency core cooling"
Topical meeting on reactor safety aspects of fuel behaviour, August 2-6, 1981, Sun Valley, Idaho, USA

[8] B.D. Clay, T. Healey and G.B. Redding
"Deformation and rupture of transiently heated Zircaloy tube"
Paper submitted to the Specialist's Meeting on the behaviour of water reactor fuel elements under accident conditions. Spaatind, Norway 12th-16th September 1976, pp. 25-27

[9] F. Erbacher, H.J. Neitzel et al.
"Out-of-pile experiments of ballooning in Zircaloy fuel rod claddings in the low pressure phase of a LOCA"
Specialist's Meeting on the behaviour of water reactor fuel elements under accident conditions. Spaatind, Norway 12th-16th September 1976, pp. 56-69

[10] F. Erbacher, H.J. Neitzel, K. Wiehr
"Studies on Zircaloy fuel clad ballooning in a LOCA, results of burst tests with indirectly heated fuel rod simulators"
Proceedings of the fourth international conference on Zirconium in the nuclear industry, ASTM, June 26-29, 1978, Stratford-on-Avon, England, ASTM-STP 681, pp. 429-445

Table 1: Argentine Cladding

Test number	Burst pressure (bar)	Burst temp. (°C)	Burst strain (%)	Burst stress (MPa)	Axial strain (%)	Time to burst (sec)
1	40	832	84	39	0.66	450
2	40	820	70	39	0.0	442
3	40	838	106	39	- 6.5	450
4	54	776	99	53	- 11.3	399
5	54	768	76	53	- 11.3	398
6	54	788	> 71	53	- 6.0	407
7	67	758	107	66	- 14.5	376
8	67	764	85	66	- 10.2	382
9	67	757		66	- 5.5	
10	80	724	74	78.5	- 10.8	348
11	80	727	72	78.5	- 4.3	358
12	80	724	76	78.5	- 6.0	351
13	94	710	70	92	- 3.3	337
14	94	715	78	92	- 7.3	339
15	94	709	67	92	- 5.3	341
16	27	887	80	26.5	2.7	
17	27	889	55	26.5	0.17	496
18	27	889	52	26.5	0.66	497
27	98	703	74	96	- 9.67	330
28	47	794	102	46	- 7.83	415
29	23	901	45	22.6	0.33	515
39	13.4	958	68	13.1	2.3	545
40	13.4	960	56	13.1	3.2	555
41	6.5	1012	26	6.4	5.2	608
42	6.5	1008	24	6.4	5.5	604

Table 2: NRG Cladding

Test number	Burst pressure (bar)	Burst temp. (°C)	Burst strain (%)	Burst stress (MPa)	Axial strain (%)	Time to burst (sec)
1	40	811	73	39	- 1.3	420
2	40	798	82	39	- 0.5	416
3	40	816	88	39	- 4.8	431
4	54	778	93	53	- 3.8	401
5	54			53	- 3.5	
6	54	772	69	53	- 0.33	404
7	64	740	67	63	- 0.33	366
8	67	755	72	66	- 7.5	372
9	67	744	76	66	- 3.0	377
10	67	734	77	66	- 0.67	370
11	80	7231	79	78.5	- 2.0	354
12	80	727	76	78.5	- 2.67	348
13	80	727	89	78.5	- 8.0	336
14	94	707	77	92	- 5.0	332
15	94	709	86	92	- 8.5	333
16	94	708	72	92	- 1.0	336
17	27	877	60	26.5	2.8	490
18	27	887	63	26.5	2.2	502
19	27	889	60	26.5	2.3	500

Table 3: Argentine Cladding

Test number	Burst pressure (bar)	Burst temp. (°C)	Burst strain (%)	A.T.D. (°C)
19A	65.6	717	25	33
20A	67	717	35.3	21
21A	42.5	783	28.7	41
22A	42.7	784	35.7	16
23A	43	813	> 28.2	58
24A	42.7	801	27	49
25A	64	798	36	33

NRG Cladding

Test number	Burst pressure (bar)	Burst temp. (°C)	Burst strain (%)	A.T.D. (°C)
21G	66.6	729	42	41
22G	66.8	754	49	70
23G	42.5	777	60	23
24G	42.3	773	> 40	14
25G	42.5	784	52	22
26G	42.5	774	70	11
27G	42.8	794	47.5	28
29G	42.8	777	55	34
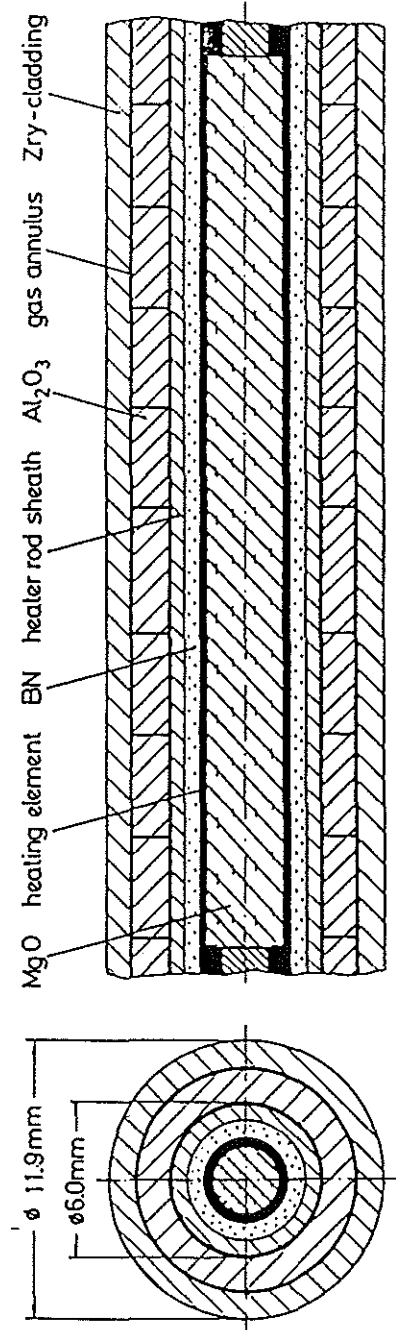
Fig. 1: Fuel rod simulator design.
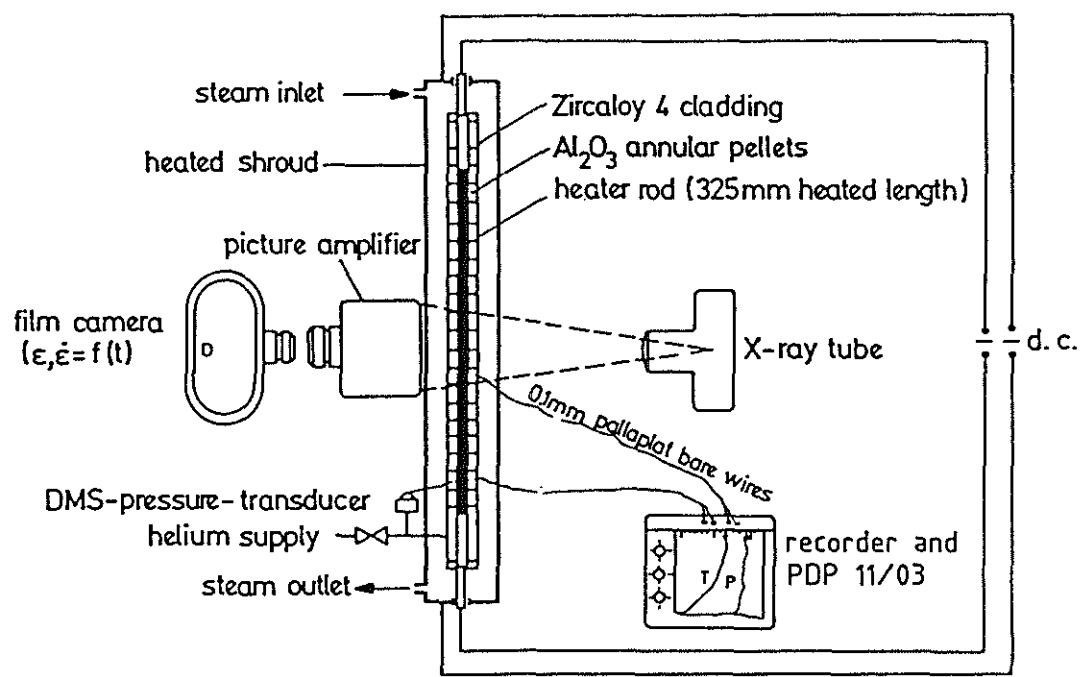
Fig. 2: Diagram of the test apparatus.

steam inlet

heated shroud

picture amplifier

film camera
$(\varepsilon, \dot{\varepsilon} = f(t))$

DMS-pressure-transducer

helium supply

steam outlet

Zircaloy 4 cladding

Al_2O_3 annular pellets

heater rod (325mm heated length)

X-ray tube

0.1mm pallaplat bare wires

recorder and
PDP 11/03

d. c.
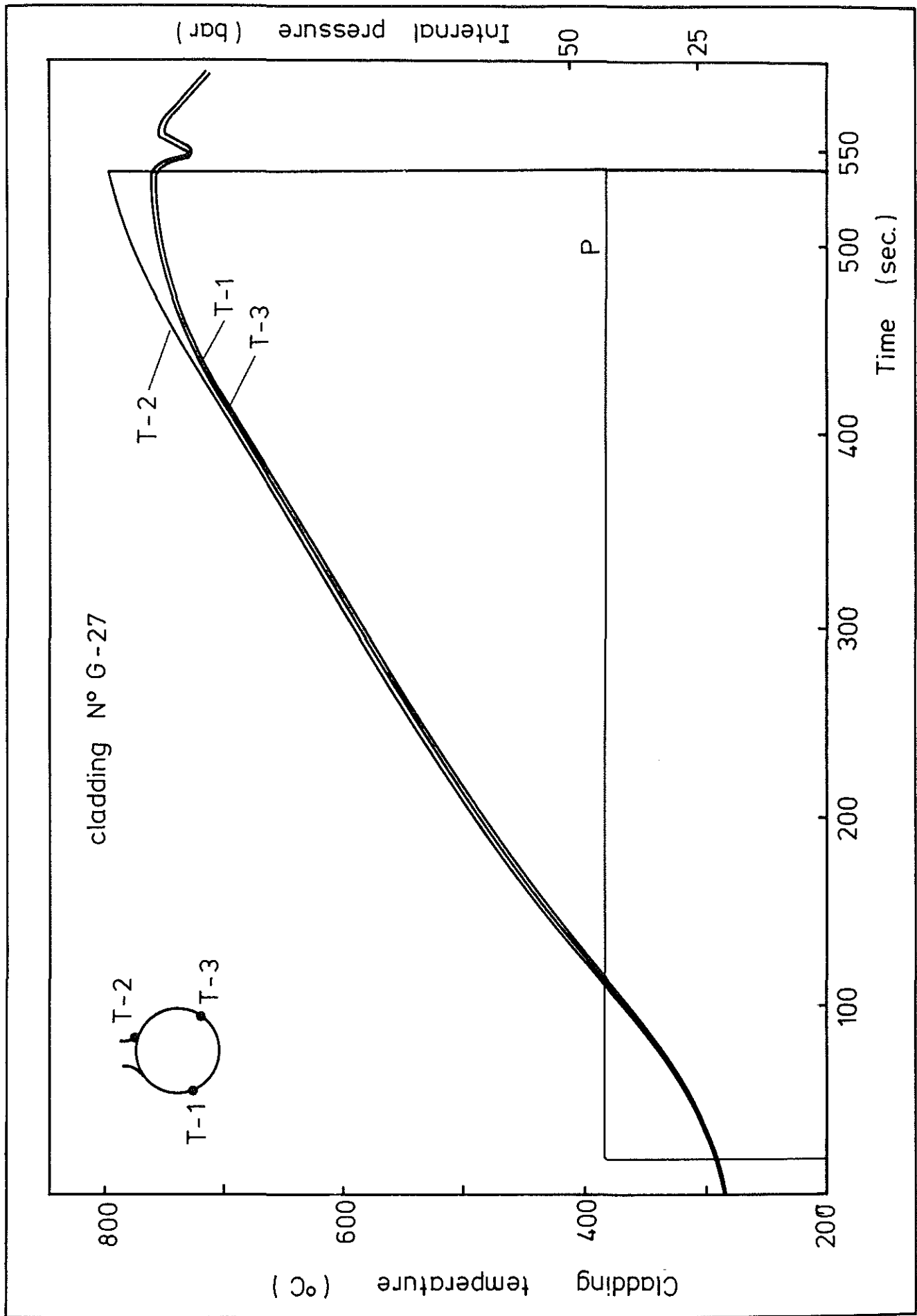
Fig. 3: Typical temperature and pressure histories and azimuthal temperature distribution during ballooning.
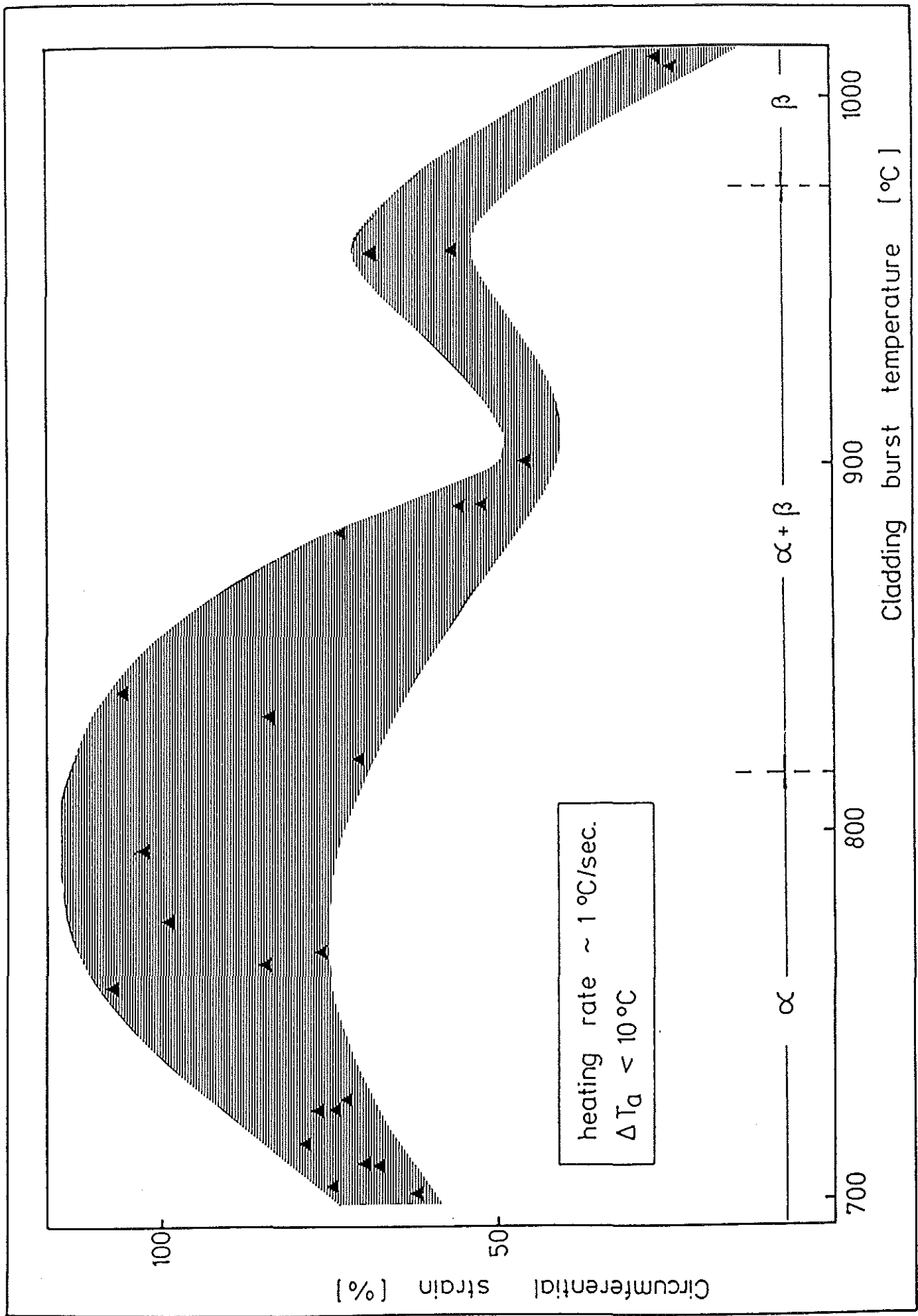
Fig. 4: Circumferential strain versus burst temperature.
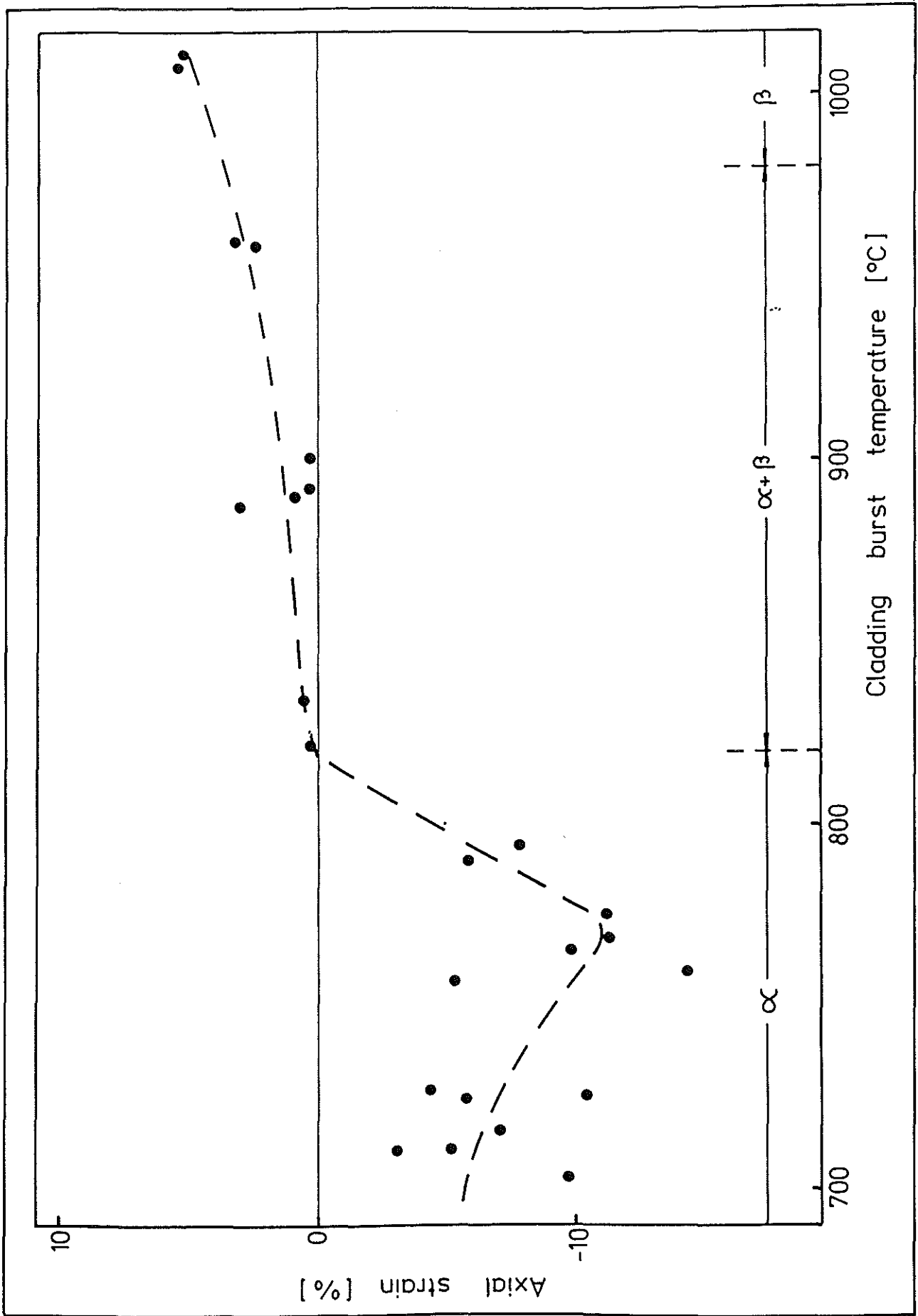
Fig. 5:   Change in axial strain as a function of burst temperature.
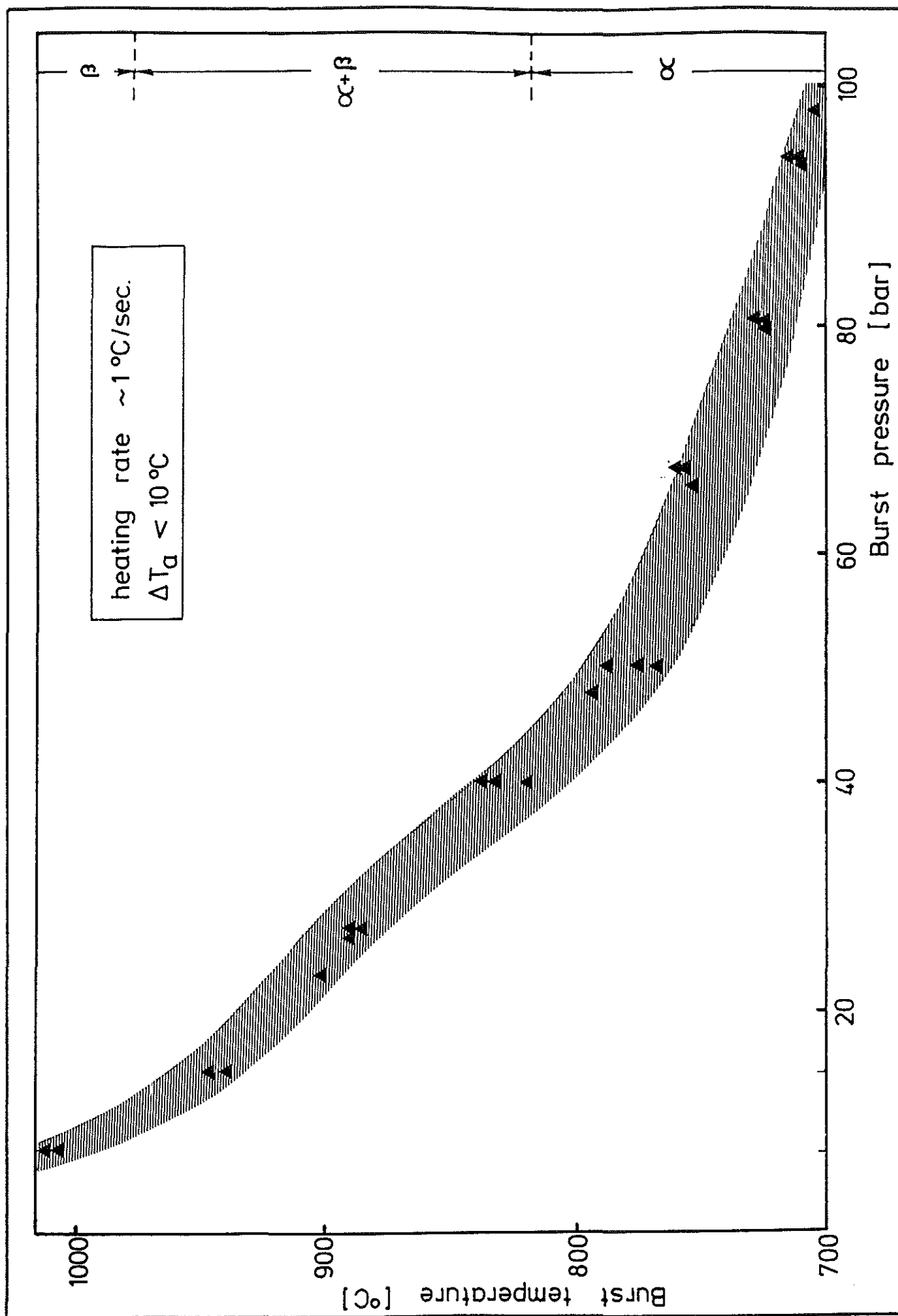
Fig. 6:   Dependence of burst temperature on burst pressure.

T_b [°C]	709	758	820	889	958	1012
P [bar]	94	67	40	27	13	6,5
Spec. N°	15	7	2	17	39	41
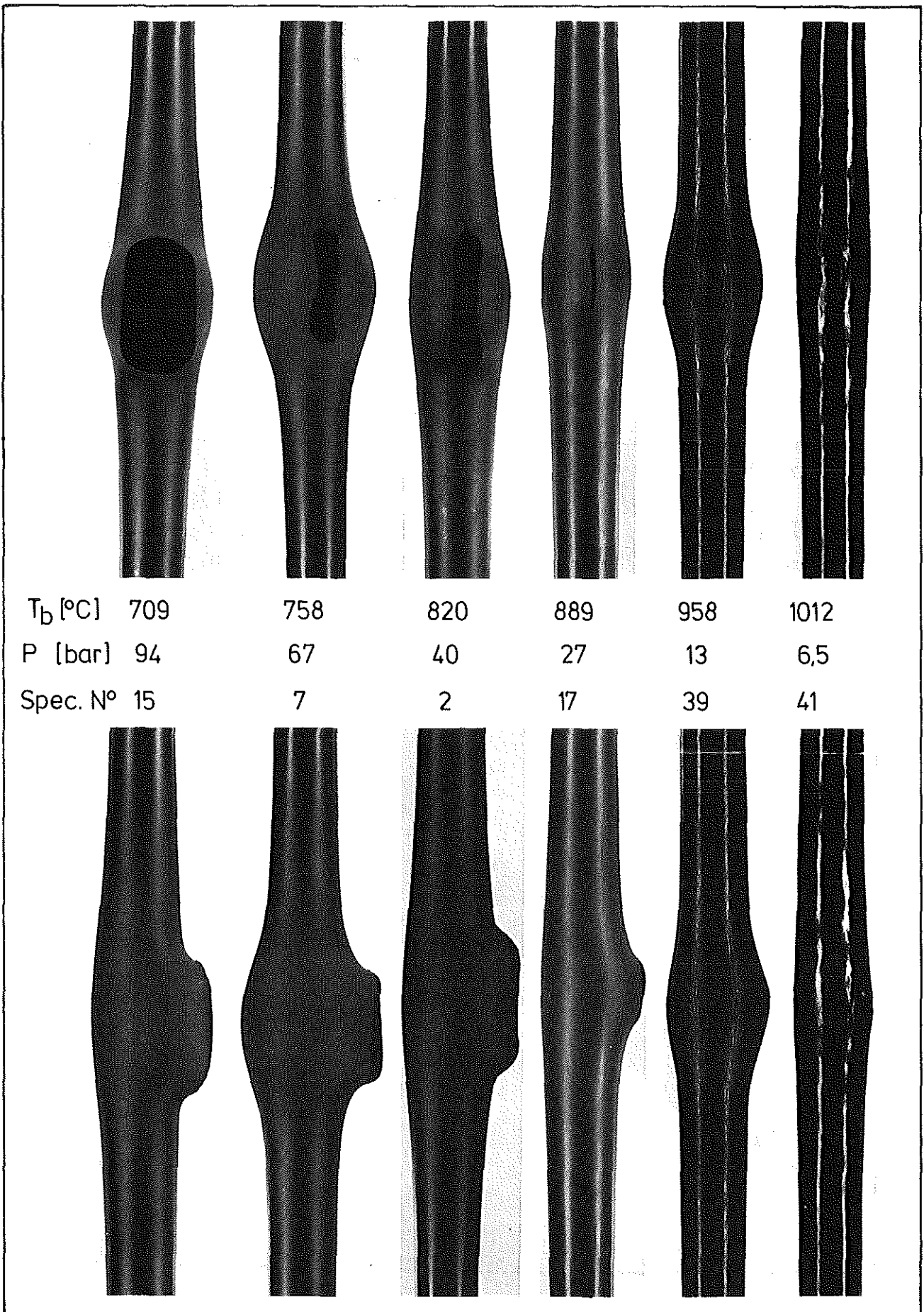
Fig. 7: Typical failure mode at different burst temperatures.

Fig. 8: Circumferential strain distribution of the ruptured region.

A-3 : bust temp. = 838 °C
A-13 : burst temp. = 710 °C
A-18 : burst temp. = 889 °C
A-41 : burst temp. = 1012 °C

Circumferential strain (%)

Distance at both side from rupture midplane (cm.)
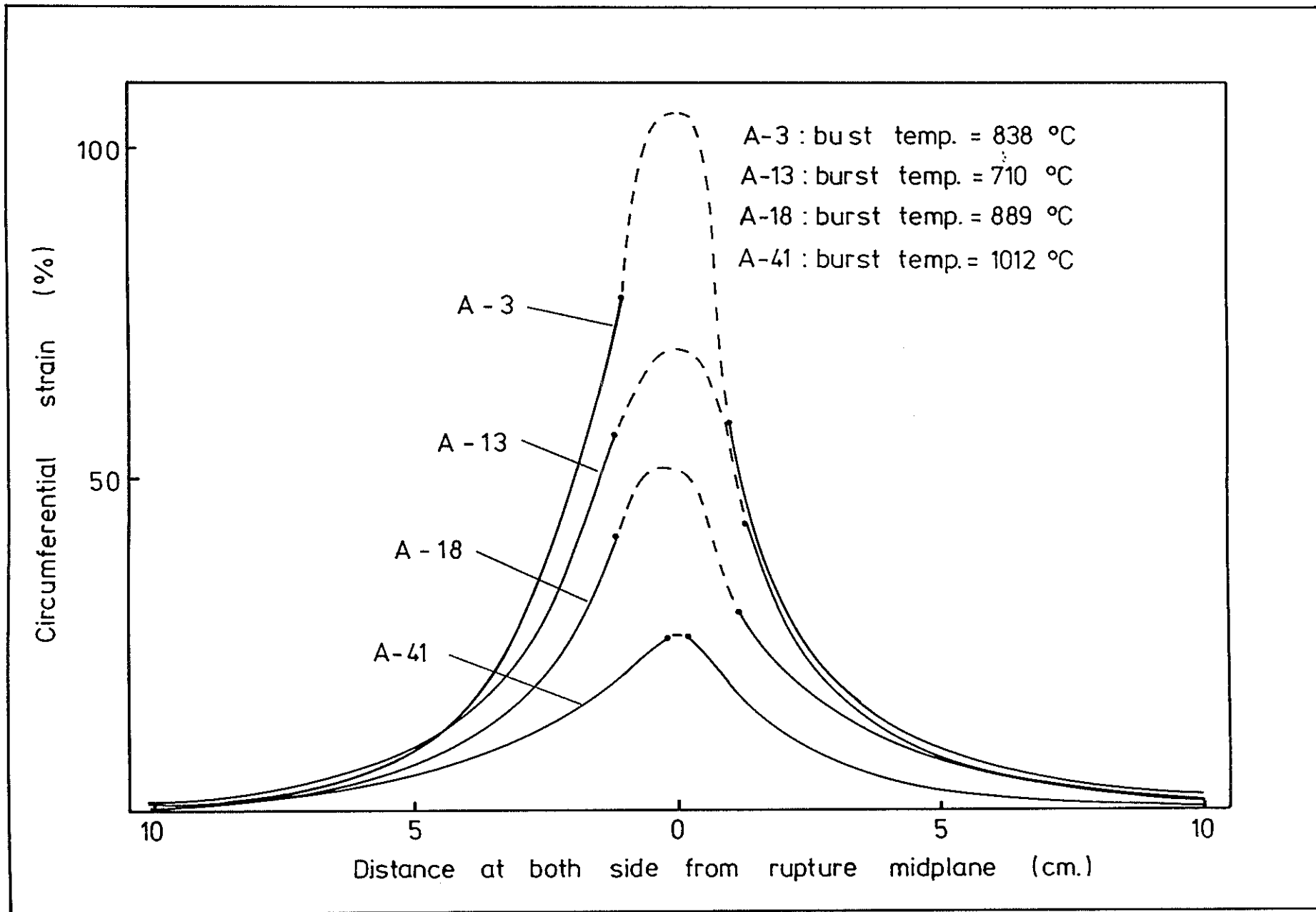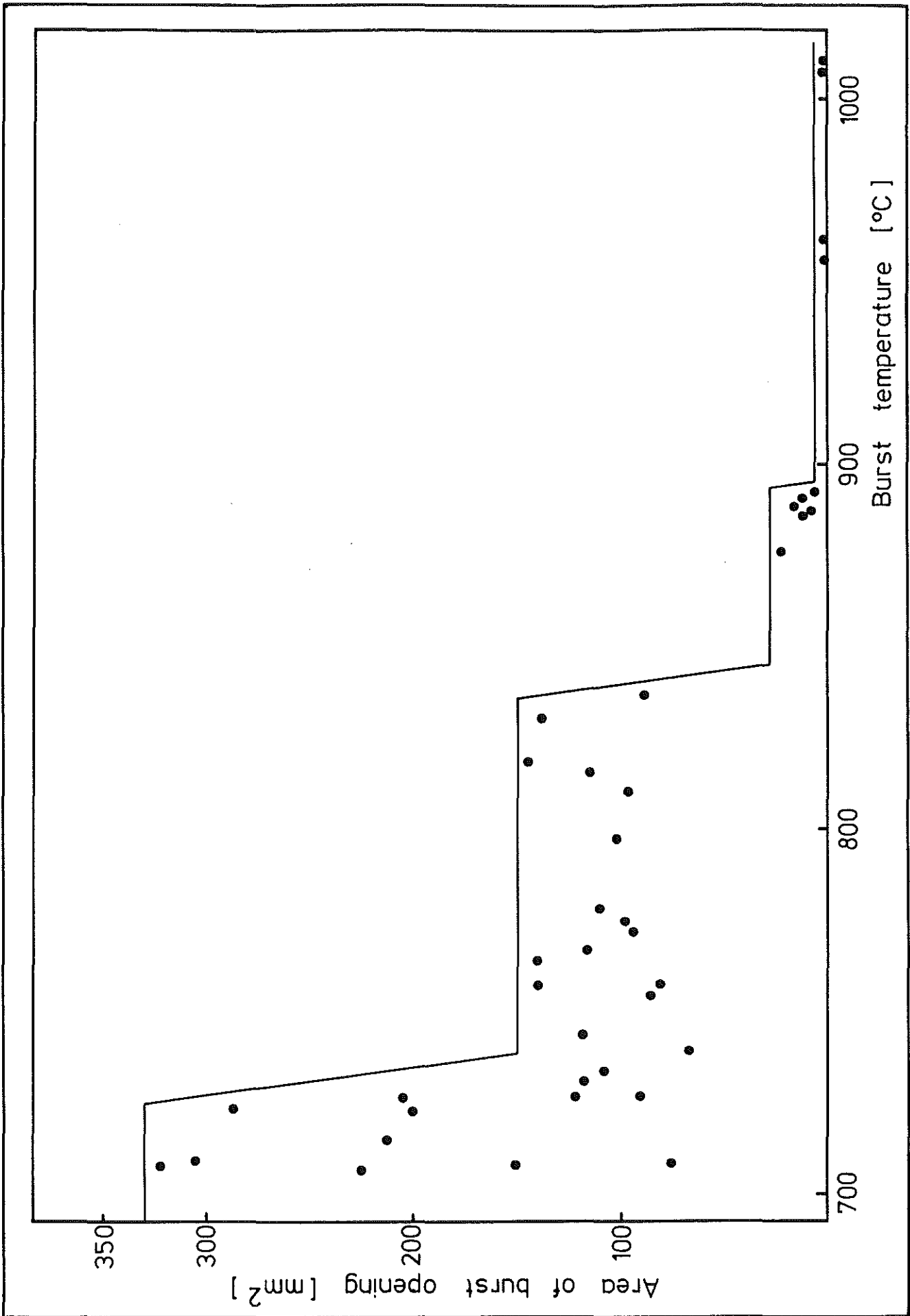
Fig. 9: Area of burst opening versus burst temperature.
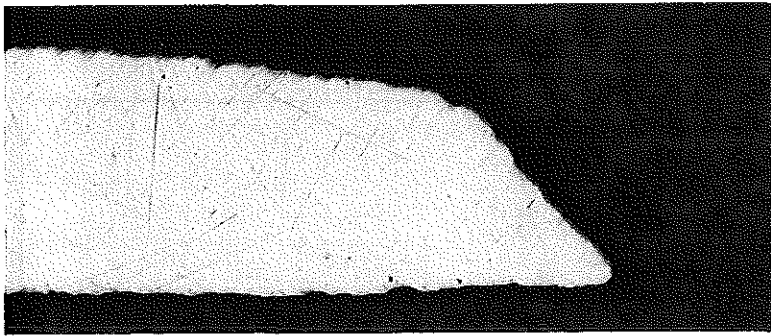
$T_b = 710\ ^{\circ}C$
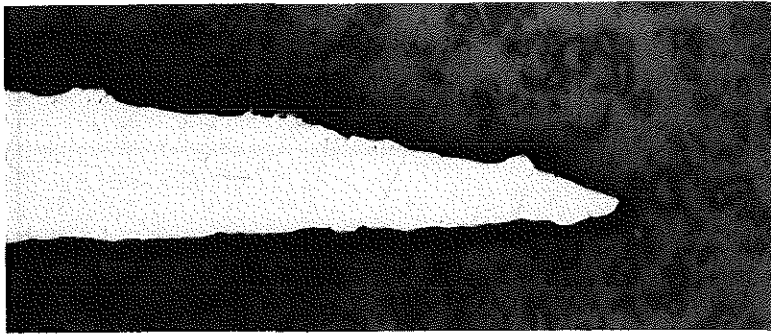
$T_b = 890\ ^{\circ}C$
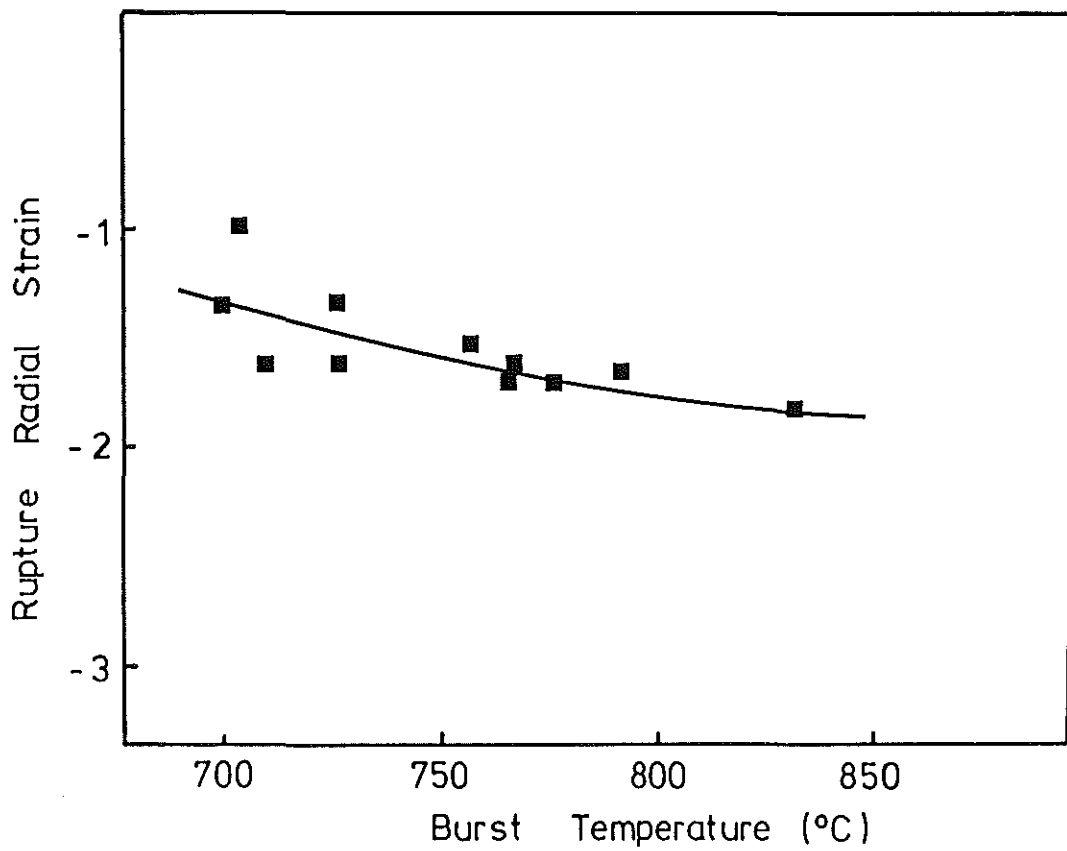
Fig. 10: Rupture radial strain versus burst temperature and tip burst orientation for failure in α and $\alpha + \beta$ phase.
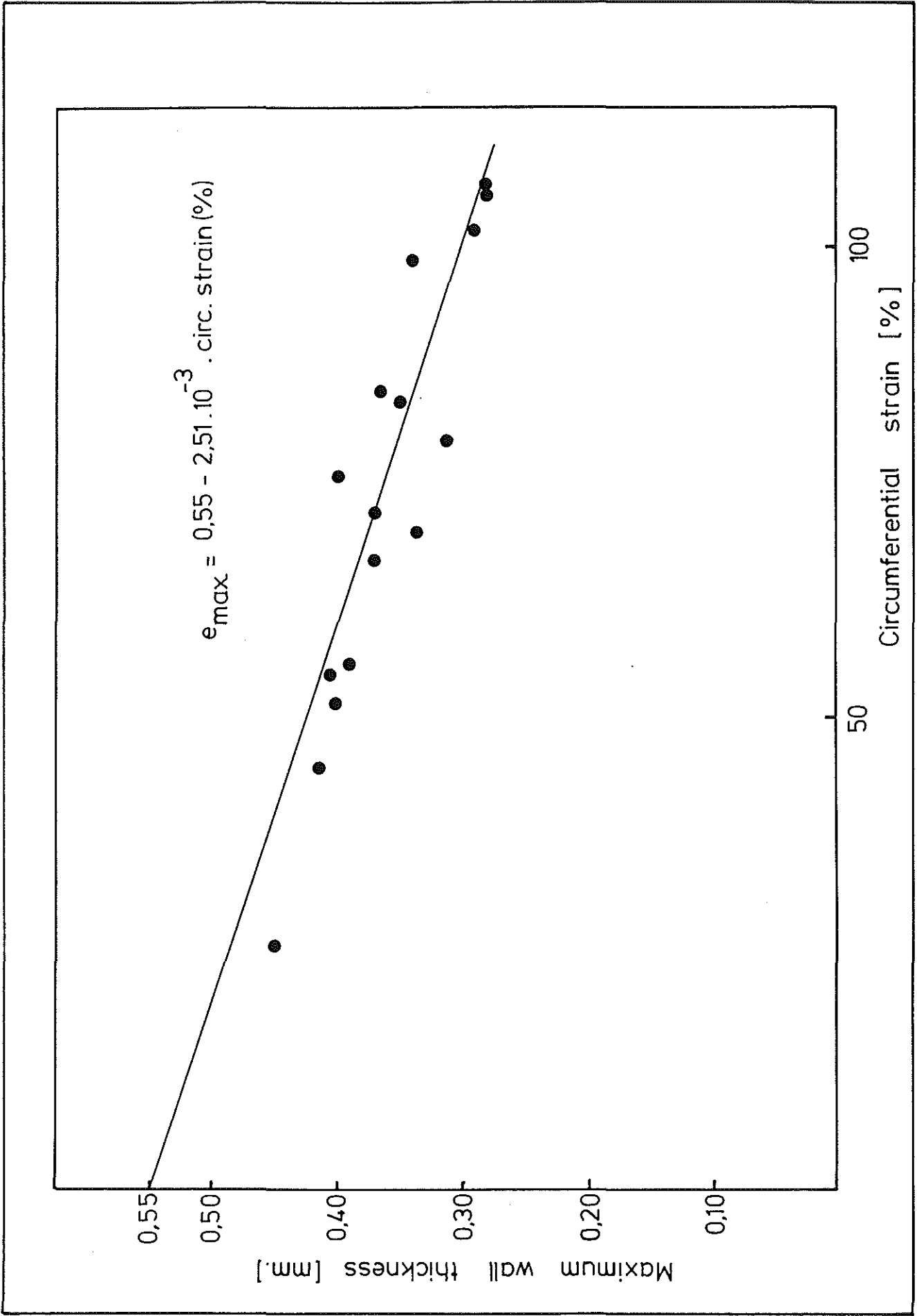
Fig. 11: Post test wall thickness measurement versus circumferential strain.

$$e_{max} = 0.55 - 2.51 \cdot 10^{-3} \cdot circ. \; strain \; (\%)$$

O. D.

I. D.

$T_b = 958\,°C$

O. D.

I. D

$T_b = 1012\,°C$
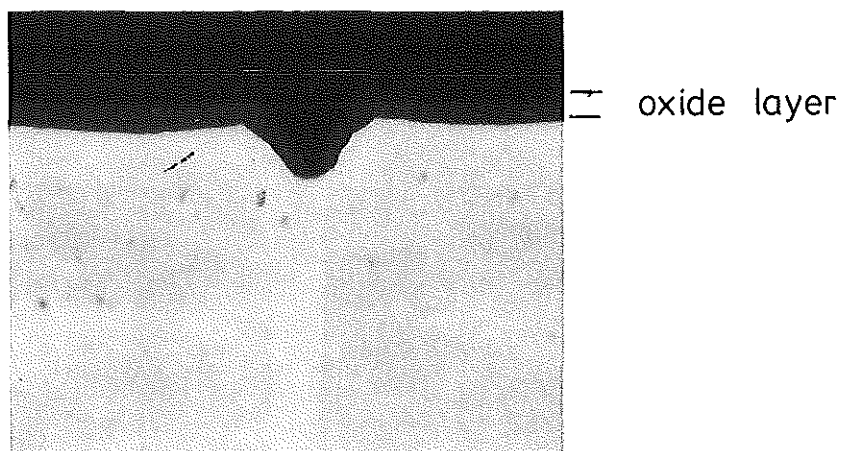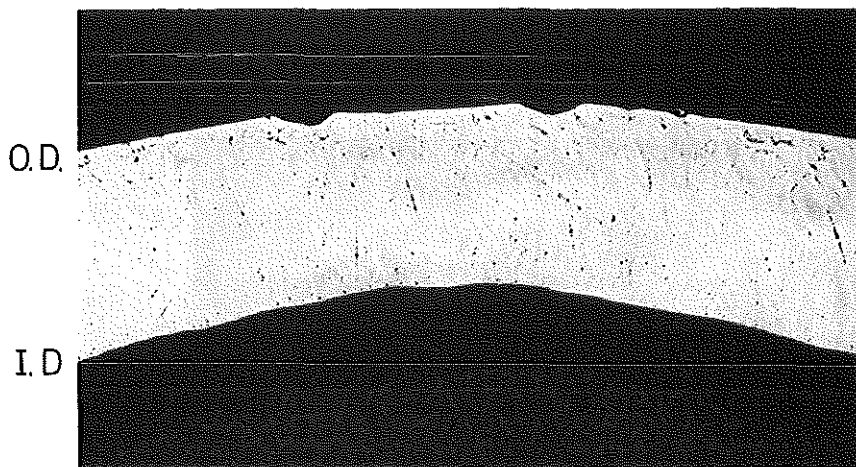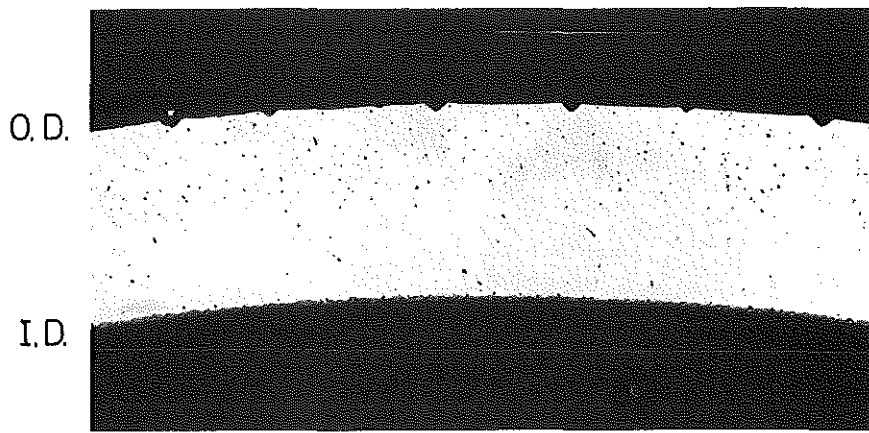
oxide layer

Fig. 12: Cracks in the oxide layer due to deformation.

cracks

O.D.

I.D.

necking

O.D.

I.D.
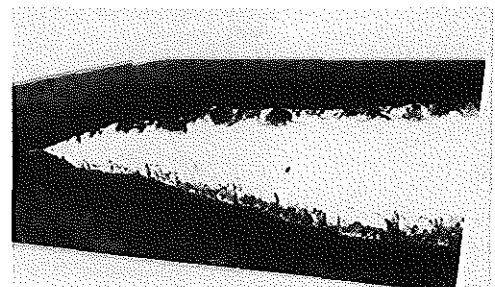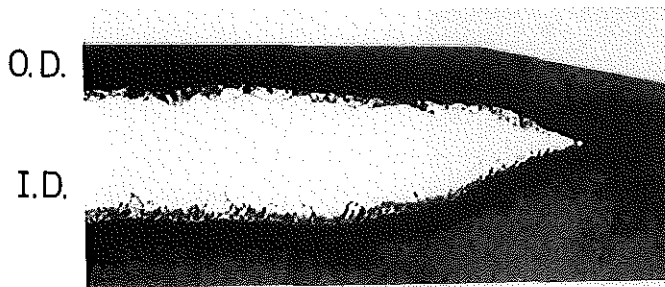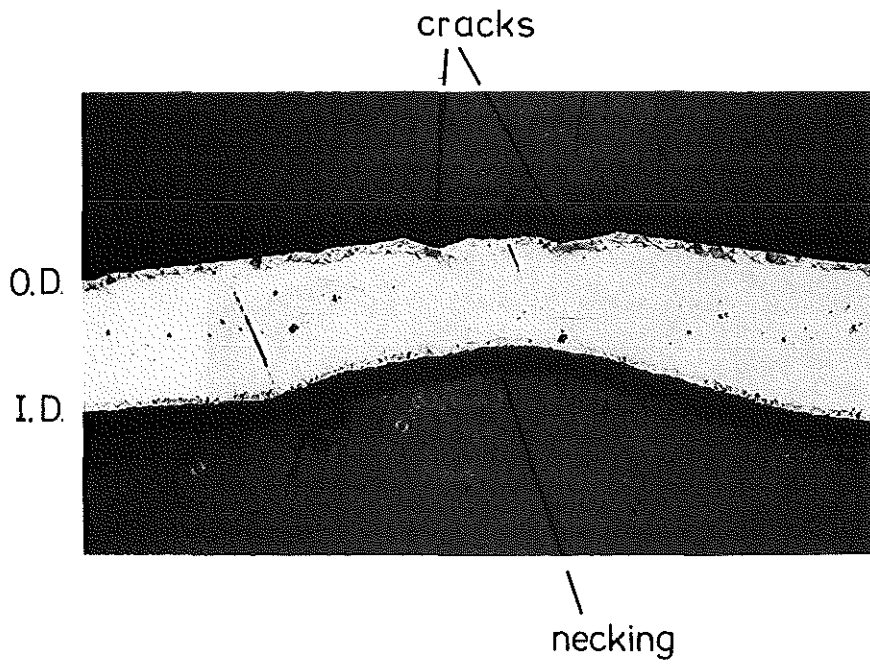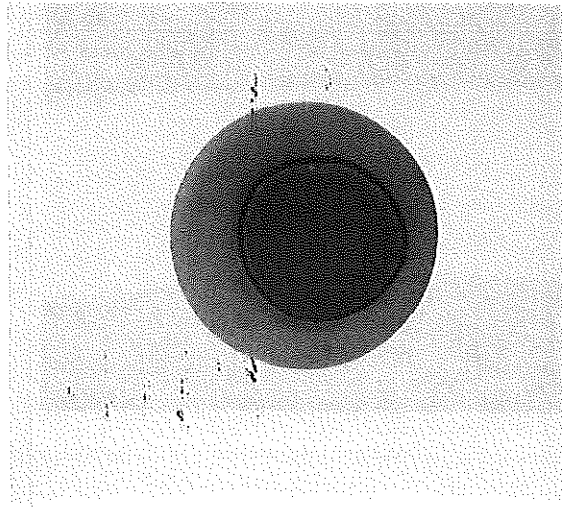
Fig. 13: Effect of oxide layer cracks on the deformation in the low β phase.
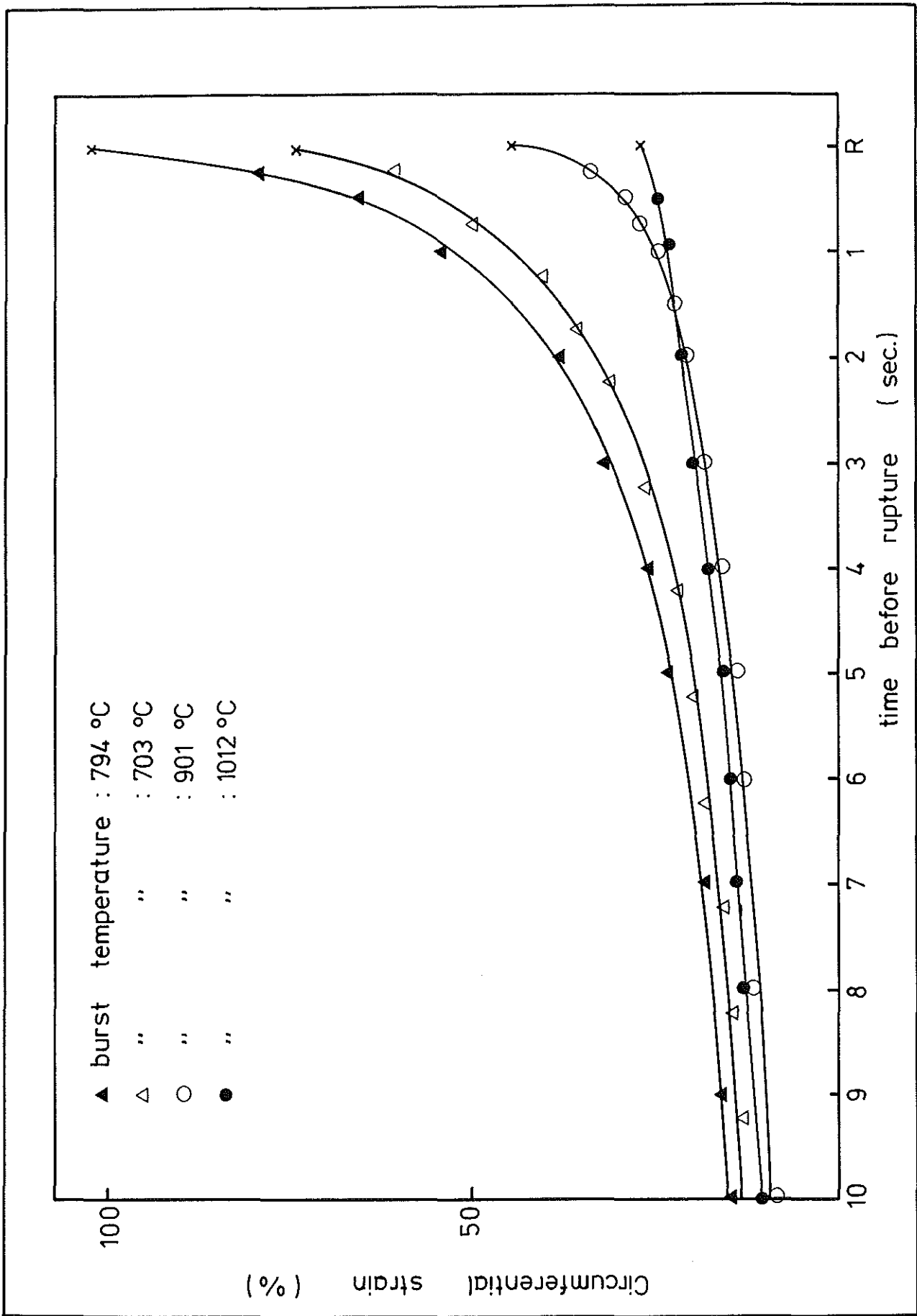
Fig. 14: Circumferential strain history versus time before rupture.

$\Delta T_{az} = 3\,°C$ $\Delta T_{az} = 58\,°C$

$\varepsilon_b = 106\,\%$ $\varepsilon_b = 28\,\%$
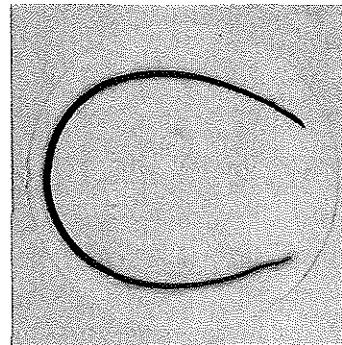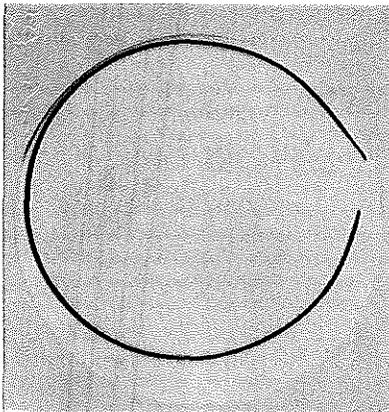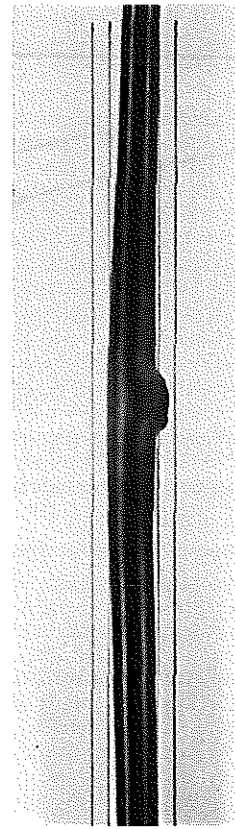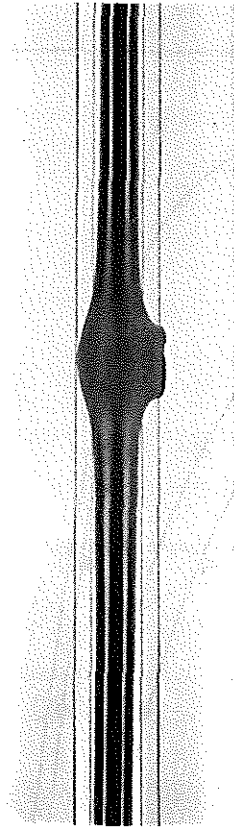
$P_b = 40\ bar$ $P_b = 42\ bar$

Fig. 15: Longitudinal and ruptured corss section view of specimens with different azimuthal temperature difference.
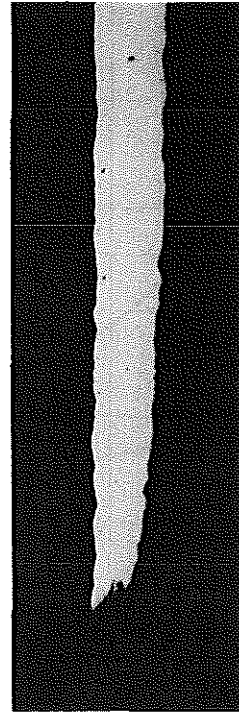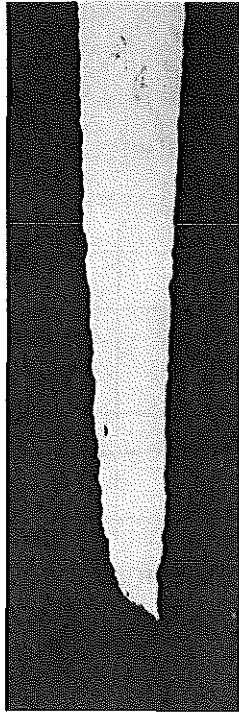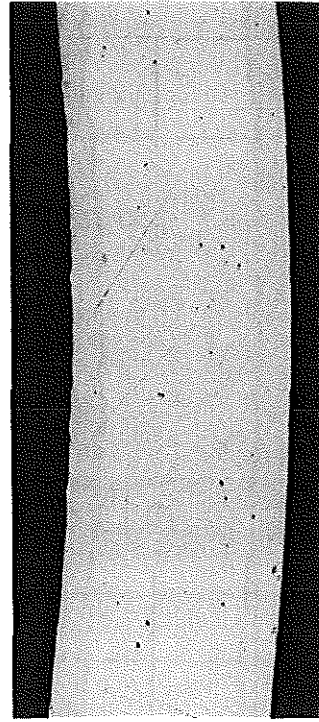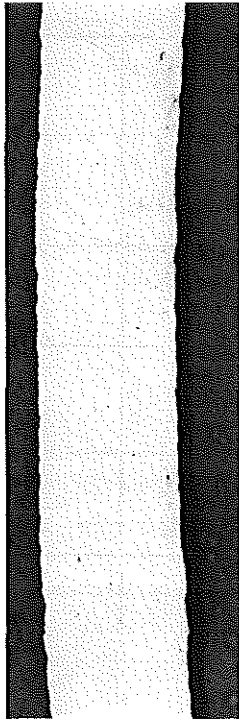
$$T_b = 838\ ^\circ C \qquad\qquad T_b = 813\ ^\circ C$$

$$\Delta T_{az} = 3\ ^\circ C \qquad\qquad \Delta T_{az} = 58\ ^\circ C$$

$$\varepsilon_b = 106\ \% \qquad\qquad \varepsilon_b = 28\ \%$$

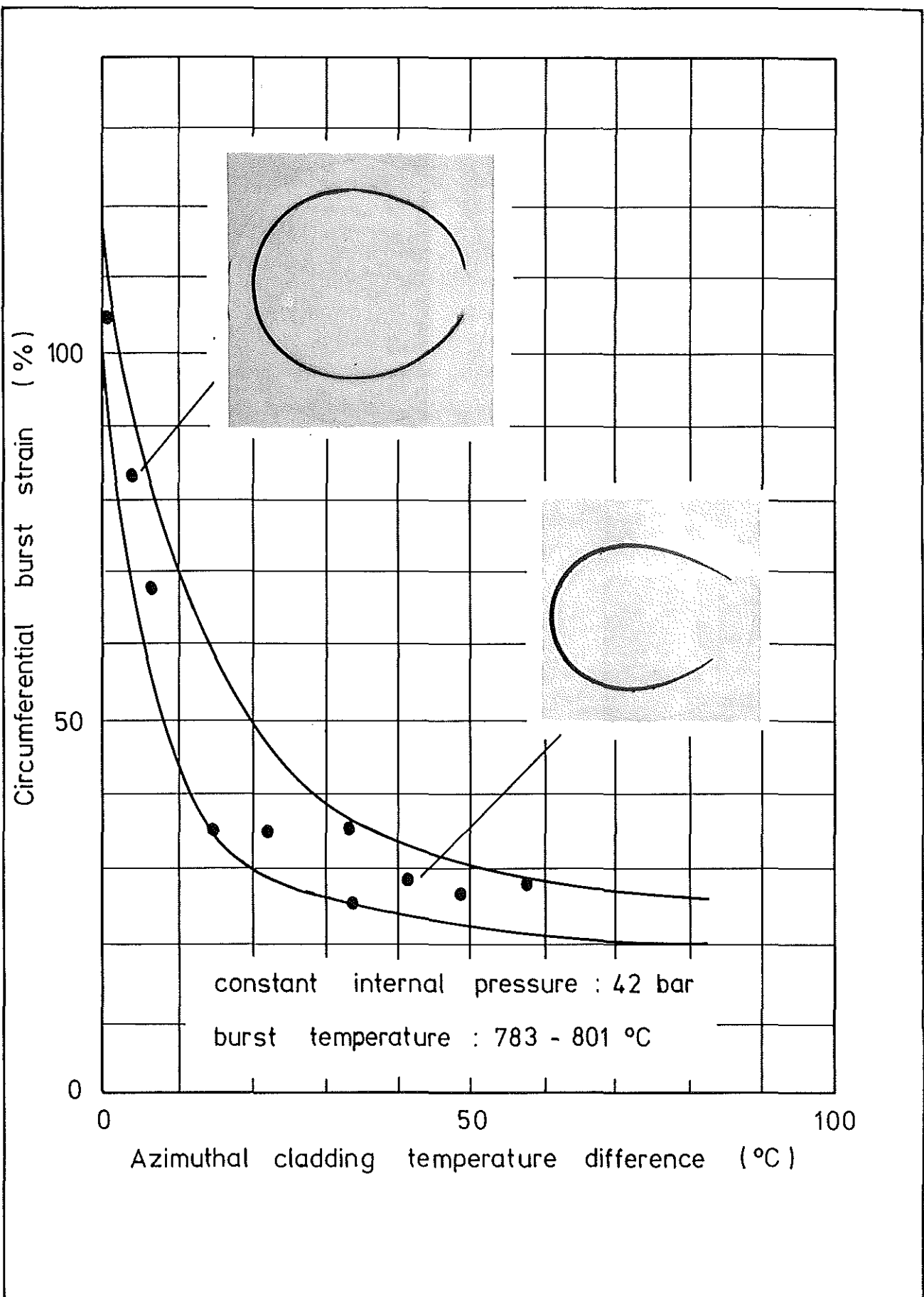**Fig. 16:** Effect of azimuthal temperature difference on wall thinning.

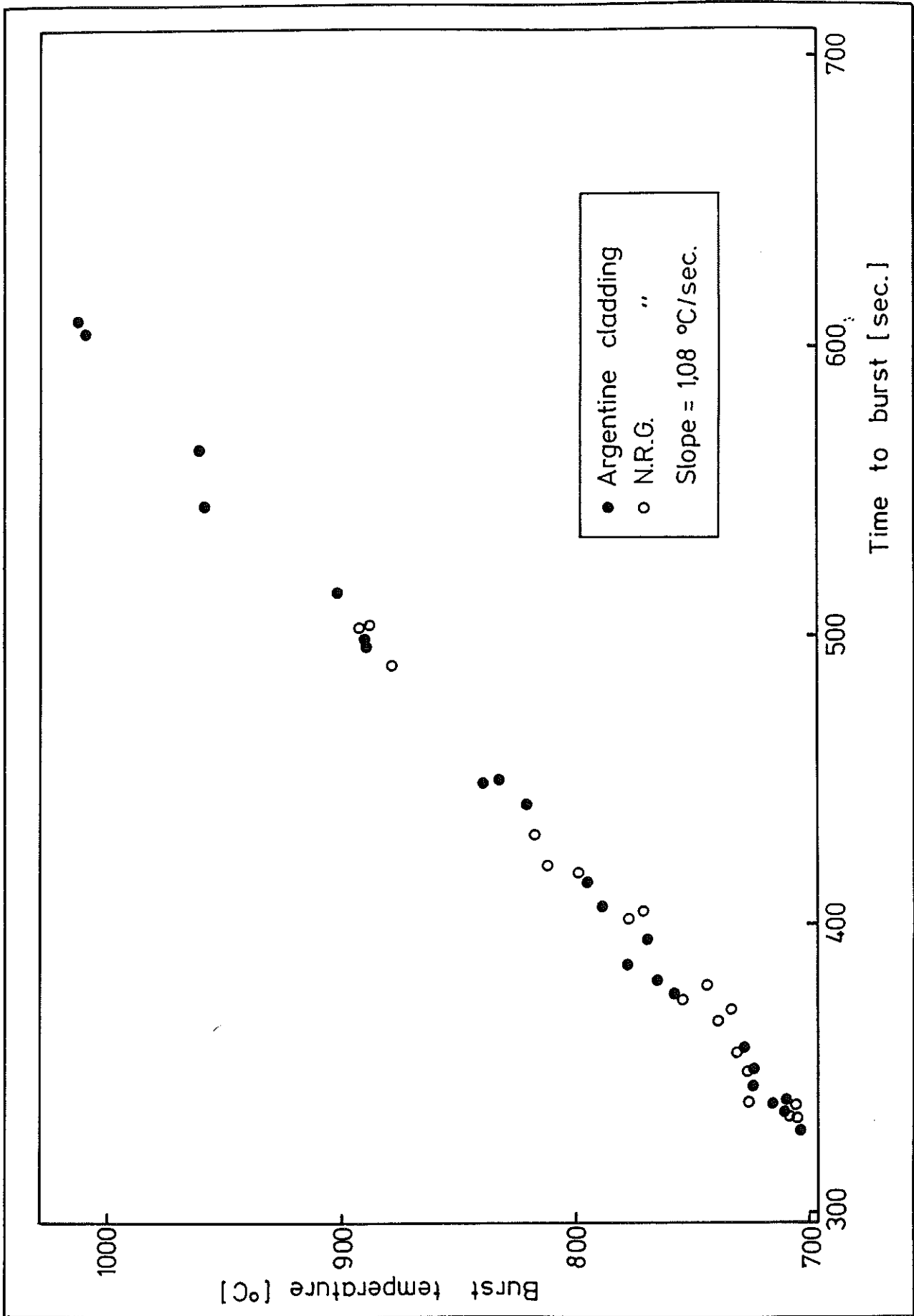Fig. 17: Burst strain versus azimuthal temperature difference.

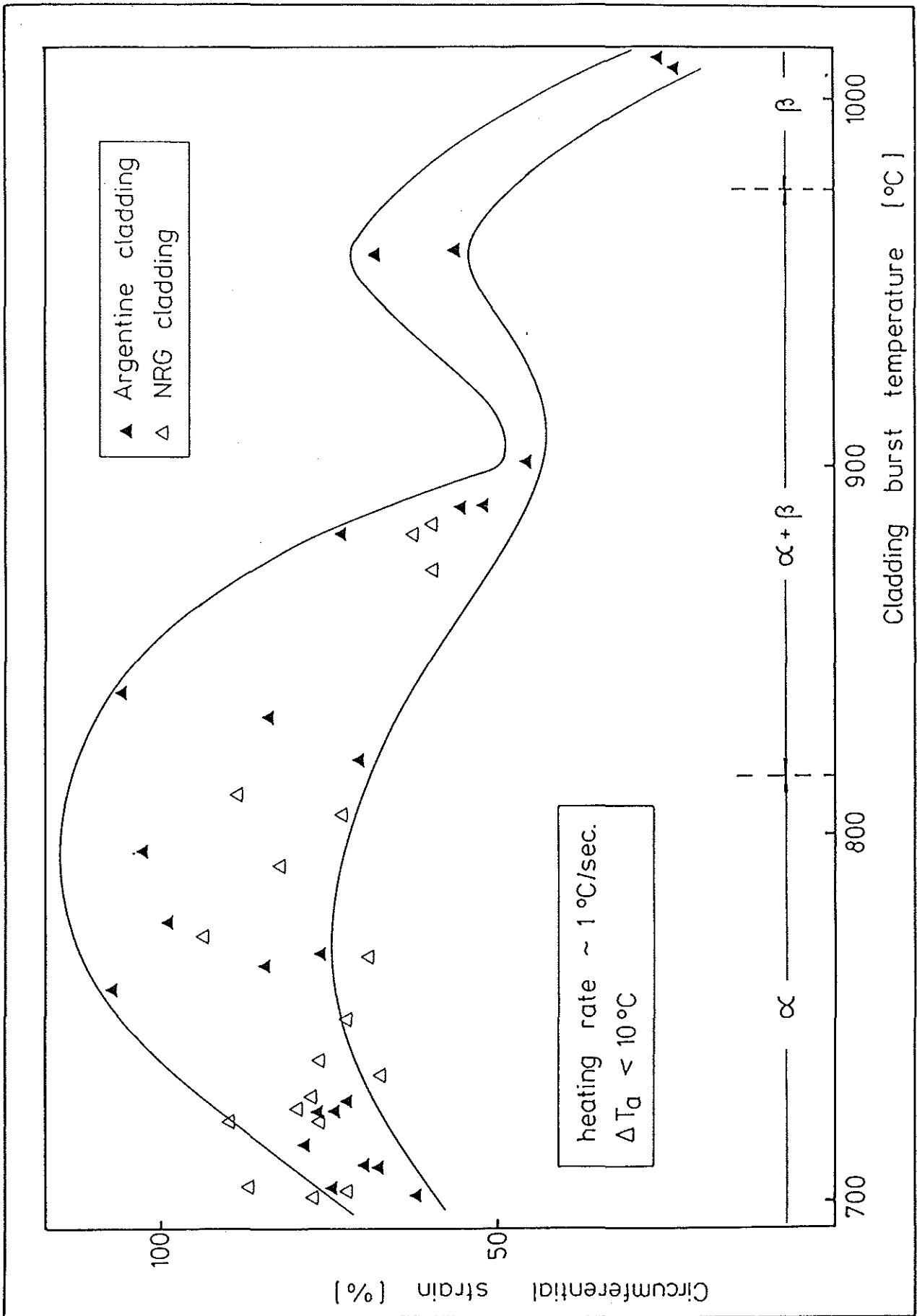Fig. 18: Burst temperature versus time to failure.

Fig. 19: Circumferential strain versus cladding burst temperature for Argentine and NRG cladding.
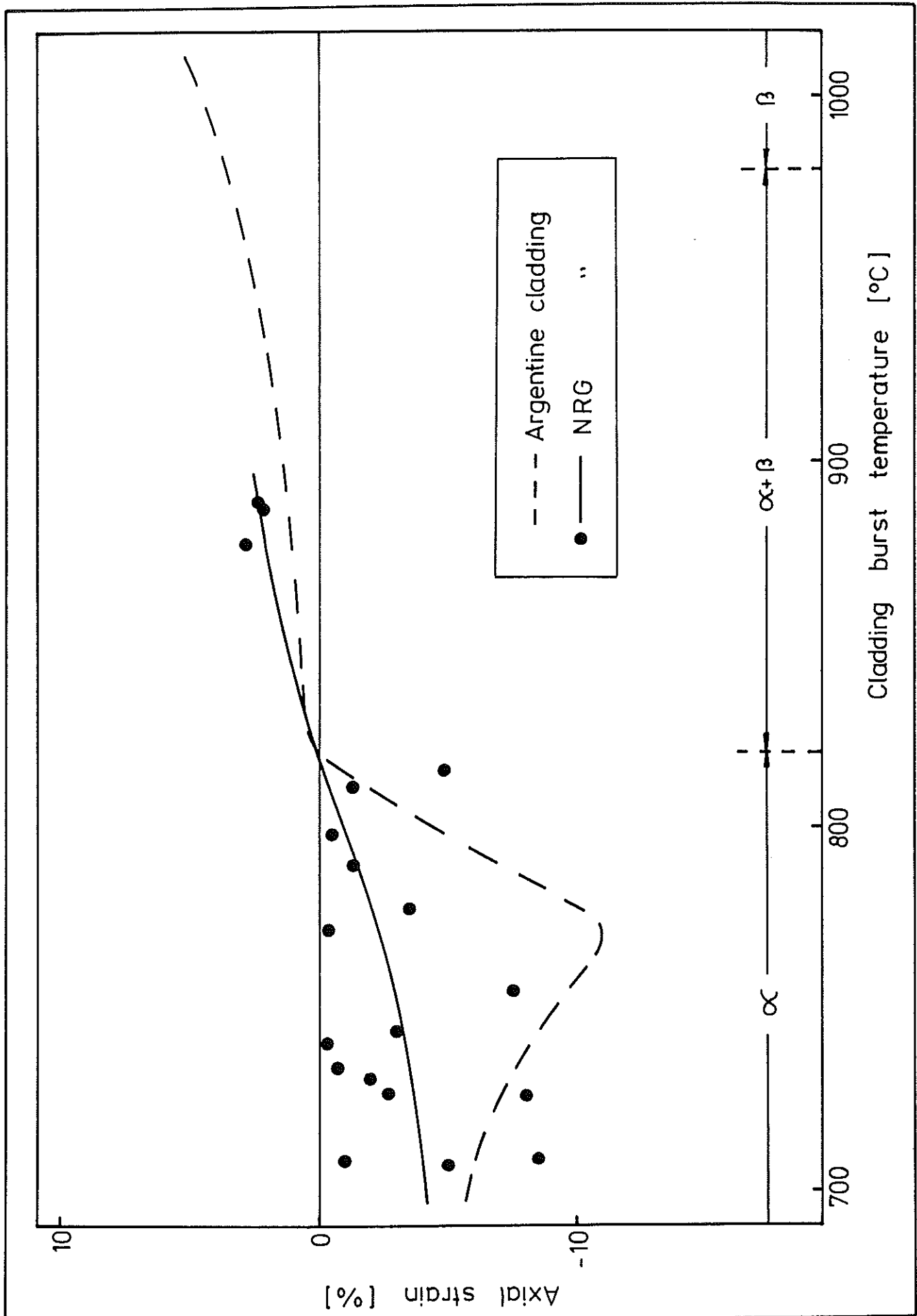
Fig. 20: Burst temperature versus burst pressure for Argentine and NRG cladding.

Fig. 21: Comparison of axial strain versus temperature for Argentine and NRG
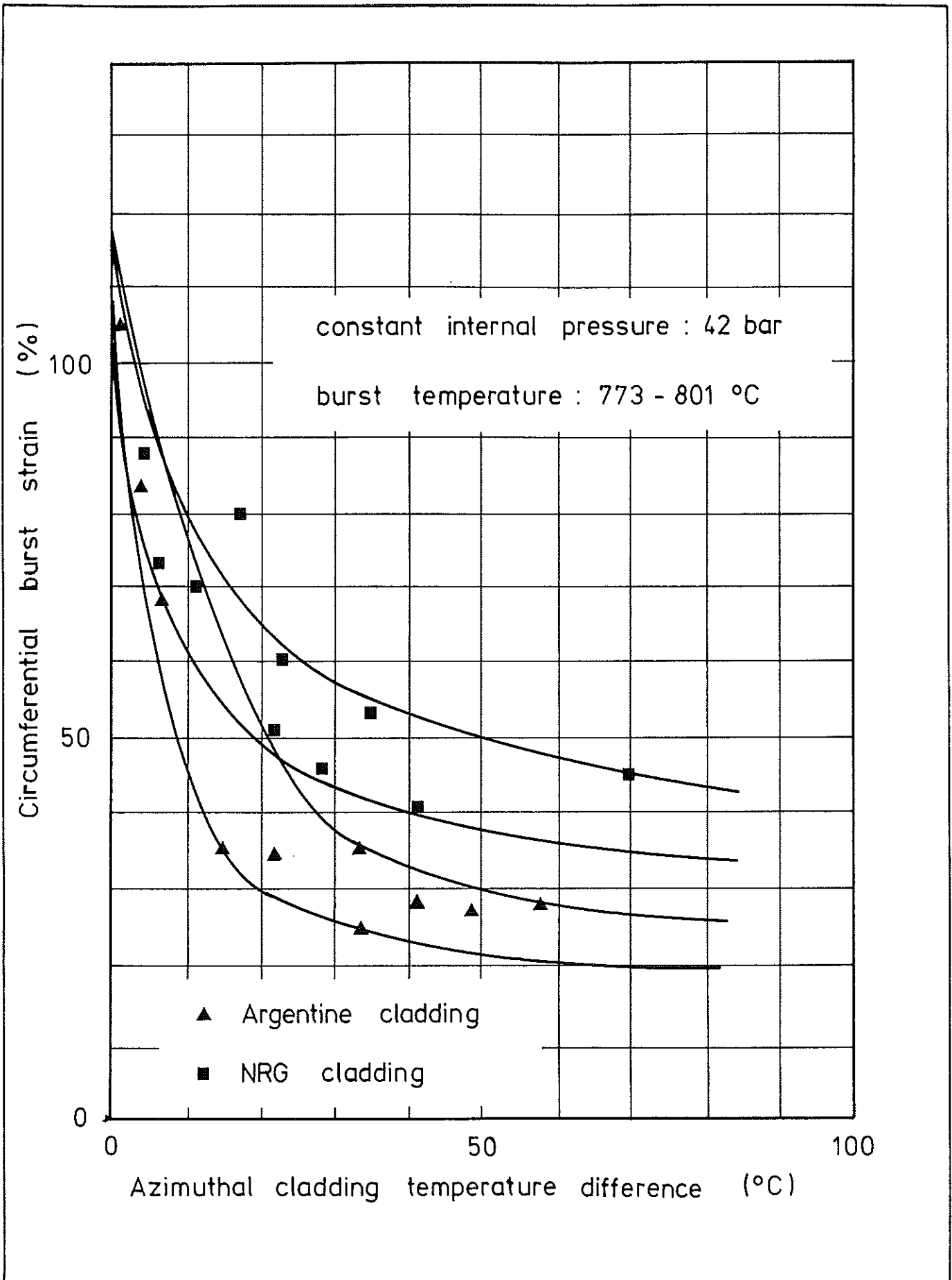cladding.

Fig. 22: Influence of non-uniformities in temperatures on the total strain for Argentine and NRG cladding.